



## Signals of Bose Einstein condensation and Fermi quenching in the decay of hot nuclear systems



P. Marini<sup>a,\*,1</sup>, H. Zheng<sup>b,c</sup>, M. Boisjoli<sup>a,d</sup>, G. Verde<sup>e,f</sup>, A. Chbihi<sup>a</sup>, P. Napolitani<sup>e</sup>, G. Ademard<sup>e</sup>, L. Augey<sup>g</sup>, C. Bhattacharya<sup>h</sup>, B. Borderie<sup>e</sup>, R. Bougault<sup>g</sup>, J.D. Frankland<sup>a</sup>, Q. Fable<sup>a</sup>, E. Galichet<sup>e,i</sup>, D. Gruyer<sup>a</sup>, S. Kundu<sup>h</sup>, M. La Commara<sup>j,k</sup>, I. Lombardo<sup>j,k</sup>, O. Lopez<sup>g</sup>, G. Mukherjee<sup>h</sup>, M. Parlog<sup>g,l</sup>, M.F. Rivet<sup>e,2</sup>, E. Rosato<sup>j,k,2</sup>, R. Roy<sup>d</sup>, G. Spadaccini<sup>j,k</sup>, M. Vigilante<sup>j,k</sup>, P.C. Wigg<sup>m</sup>, A. Bonasera<sup>b,c</sup>  
(INDRA Collaboration)

<sup>a</sup> Grand Accélérateur National d'Ions Lourds, Bd. Henri Becquerel, BP 55027, 14076 Caen, France

<sup>b</sup> Cyclotron Institute, Texas A&M University, College Station, TX-77843, USA

<sup>c</sup> Laboratori Nazionali del Sud, INFN, via Santa Sofia, 62, 95123 Catania, Italy

<sup>d</sup> Laboratoire de Physique Nucléaire, Université Laval, Québec, G1V 0A6, Canada

<sup>e</sup> Institut de Physique Nucléaire, CNRS-IN2P3, Univ. Paris-Sud, Université Paris-Saclay, 91406 Orsay Cedex, France

<sup>f</sup> INFN – Sezione di Catania, via Santa Sofia, 64, 95123 Catania, Italy

<sup>g</sup> Laboratoire de Physique Corpusculaire, ENSICAEN, Université de Caen Basse Normandie, CNRS/IN2P3, F-14050 Caen Cedex, France

<sup>h</sup> Variable Energy Cyclotron Center, Kolkata, India

<sup>i</sup> Conservatoire National des Arts et Métiers, F-75141 Paris Cedex 03, France

<sup>j</sup> Dipartimento di Fisica, Università di Napoli "Federico II", Napoli, Italy

<sup>k</sup> INFN – Sezione di Napoli, Strada Comunale Cintia, 80126 Napoli, Italy

<sup>l</sup> "Horia Hulubei" National Institute of Physics and Nuclear Engineering (IFIN-HH), RO-077125 Bucharest Magurele, Romania

<sup>m</sup> University of Liverpool, School of Physical Sciences, Physics Department, Oliver Lodge Laboratory, Oxford Street, Liverpool L69 7ZE, UK

### ARTICLE INFO

#### Article history:

Received 26 June 2015

Received in revised form 11 February 2016

Accepted 26 February 2016

Available online 2 March 2016

Editor: V. Metag

#### Keywords:

Bose–Einstein condensation

Heavy ion collisions

Quantum-fluctuations method

### ABSTRACT

We report on first experimental observations of nuclear fermionic and bosonic components displaying different behaviours in the decay of hot Ca projectile-like sources produced in mid-peripheral collisions at sub-Fermi energies. The experimental setup, constituted by the coupling of the INDRA 4 $\pi$  detector array to the forward angle VAMOS magnetic spectrometer, allowed to reconstruct the mass, charge and excitation energy of the decaying hot projectile-like sources. By means of quantum-fluctuation analysis techniques, temperatures and local partial densities of bosons and fermions could be correlated to the excitation energy of the reconstructed system. The results are consistent with the production of dilute mixed systems of bosons and fermions, where bosons experience higher phase-space and energy density as compared to the surrounding fermionic gas. Our findings recall phenomena observed in the study of Bose condensates and Fermi gases in atomic traps despite the different scales.

© 2016 The Authors. Published by Elsevier B.V. This is an open access article under the CC BY license (<http://creativecommons.org/licenses/by/4.0/>). Funded by SCOAP<sup>3</sup>.

The study of quantum systems composed of bosons and fermions stimulates significant theoretical and experimental effort in different fields of physics. For instance, investigations of quantum systems presenting mixtures of bosons and fermions, with the outstanding example of <sup>3</sup>He–<sup>4</sup>He fluids, have led to the obser-

\* Corresponding author.

E-mail address: [marini@cenbg.in2p3.fr](mailto:marini@cenbg.in2p3.fr) (P. Marini).

<sup>1</sup> Present address: Centre d'Études Nucléaires de Bordeaux Gradignan, Chemin du Solarium Le Haut Vigneau, 33175 Gradignan, France.

<sup>2</sup> Deceased.

vation of Bose–Einstein condensation (BEC) and Fermi quenching (FQ) [1,2]. In nuclear-physics experiments we observe the existence of phenomena that can be explained by considering nuclei as systems whose properties are ascribed to the fact that they are composed of bosonic clusters, the most important being  $\alpha$  particles, arising from a reorganisation of their fundamental fermionic constituents, protons and neutrons [3–8]. If the nucleus is composed of fermions and bosons, one may wonder whether the bosonic properties may dominate over the fermionic properties in some instances, such as for the Hoyle state in <sup>12</sup>C. Along this direction [9–11], it has been suggested that Bose-condensate sig-

natures may be observed in hot nuclei produced during heavy-ion collisions [12]. The present article aims at identifying different signals from bosons and fermions with the purpose of investigating BEC phenomena in the decay of excited quasi-projectile systems produced in semi-peripheral Ca + Ca collisions at  $E/A = 35$  MeV. The results display analogies with phenomena observed in atomic traps [2], suggesting links between atomic and nuclear physics phenomenologies.

The experiment was performed at the Grand Accélérateur National d'Ions Lourds (GANIL).  $^{40}\text{Ca}$  targets were bombarded with  $^{40}\text{Ca}$  beams at 35 MeV/nucleon. An innovative setup, constituted by 288 telescopes of the  $4\pi$  detector INDRA [13], covering angles  $\theta = 7^\circ\text{--}176^\circ$ , and by the large acceptance and high resolution VAMOS magnetic spectrometer [14] at very forward angles ( $2^\circ < \theta < 7^\circ$ ), which triggers the data acquisition, was used for this study. The combined setup [15] allowed to reconstruct the mass, charge and excitation energy of the quasi-projectile (QP) system, and to characterise its decay channels on an event-by-event basis. Such decay leaves the system with a forward moving QP residue, detected and identified in charge and mass with the VAMOS spectrometer, and coincident light particles and fragments emitted at larger angles and detected by INDRA telescopes. Only peripheral and semi-peripheral collisions, leading to a heavy QP residue with  $Z > 5$  detected in VAMOS, are discussed therein. To reconstruct the charge,  $Z_{\text{QP}}$ , mass,  $A_{\text{QP}}$ , and momentum vector,  $\vec{p}_{\text{QP}}$ , of the QP, particles with  $Z = 1, 2$  and  $Z \geq 3$ , detected by INDRA, were attributed to QP decay when their longitudinal velocities lay within the range of  $\pm 65\%$ ,  $\pm 60\%$ ,  $\pm 45\%$ , respectively, of the coincident QP residue velocity [16]. This selection is intended to remove fragments from non-QP sources [17]. To minimise contributions from entrance-channel effects, predominant in the beam direction, we have estimated the excitation energy,  $E^*/A$ , of the reconstructed QPs from the momenta ( $\vec{p}_\perp$ ) of their accompanying emitted particles transverse to the quasi-projectile momentum. This allowed to extract transverse excitation energy,  $E^*$ , through calorimetry as the sum of the charged particle transverse kinetic energy in the QP reference frame ( $K_\perp^i$ ), corrected for the reaction  $Q$ -value:  $E^* = \frac{3}{2} \sum_i K_\perp^i - Q_{\text{value}}$  [18].

Events with a reconstructed QP mass between 34 and 46 were selected, which correspond to a QP charge distribution centred at  $Z_{\text{QP}} = 20$  and with a standard deviation of about 1 unit. The reconstructed mass  $A_{\text{QP}}$  does not account for the emitted (not detected) neutrons. However, simulations performed with a statistical decay model (the code GEMINI [19] was used) show that the evaporation of Ca QPs at these measured excitation energies mostly produces an average neutron multiplicity  $M_n \lesssim 1$ . This is due to the fact that the  $\alpha$  (proton) emission is energetically favoured with respect to neutron emission for all the selected Ca isotopes heavier (lighter) than  $^{40}\text{Ca}$  (with the exception of  $^{45,46}\text{Ca}$ ). The uncertainty on  $E^*/A$  due to the non-detection of neutrons is within the chosen  $E^*/A$  bin width (0.5 MeV/nucleon) in figures displayed in this article.

Fig. 1(a) shows the measured multiplicity of different light particles as a function of the reconstructed transverse excitation energy of the QP. In panel (b) we also show the evolution of the charge,  $Z_{\text{max}}$ , of the largest fragment left by the decay of the QP, which is similar to previous works [20]. To isolate events with isotropic emission, i.e. characterised by a certain degree of equilibration, we place a selection on the longitudinal momentum ( $p_z^i$ ) and transverse momentum ( $p_\perp^i$ ) of the fragments comprising the QP:  $-0.3 \leq \log_{10}(Q_{\text{shape}}) \leq 0.3$  where  $Q_{\text{shape}} = \sum_i (p_z^i)^2 / \sum_i (p_\perp^i)^2$ , with the sum extending over all fragments of the QP. This selection allows to remove events where the kinetic-energy spectra of the emitted particles differ from an exponential and present a high energy tail, likely due to a remaining contribution from mid-rapidity emission. Among the studied particles,  $\alpha$  particles are the most af-

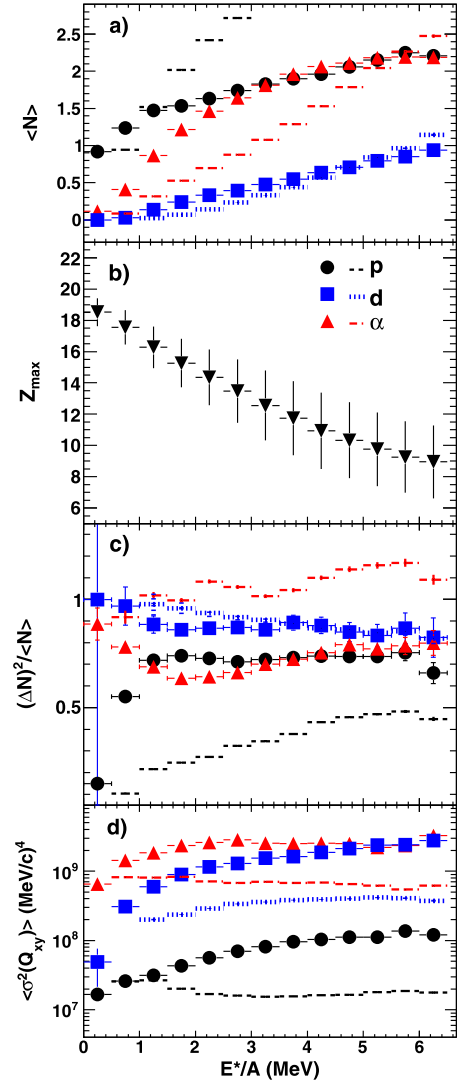


Fig. 1. (Colour online.) (a) Measured mean multiplicity of protons, deuterons and alphas; (b) charge of the largest fragment; (c) multiplicity fluctuations and (d) quadrupole momentum fluctuations of particles emitted by QPs as a function of their transverse excitation energy per nucleon,  $E^*/A$ . Results obtained for GEMINI data are shown as dotted lines.

ected by this selection. Its impact on the observables presented here (in particular temperatures and densities) will be discussed in the following.

In Fig. 1(c) we present the multiplicity fluctuations,  $(\Delta N)^2 / \langle N \rangle$ , for protons ( $p$ ), deuterons ( $d$ ) and alphas ( $\alpha$ ) as a function of  $E^*/A$ . Significant differences exist between fermions and bosons at low  $E^*$ . In a system where the quantum nature of these particles could be neglected, their multiplicity fluctuations would be at the classical limit  $(\Delta N)^2 / \langle N \rangle = 1$  [21]. However, in our data we observe that they are all below such limit. For fermions this phenomenon is known as fermion quenching and has been observed in trapped Fermi gas and heavy-ion collisions [22,23]. For bosons  $(\Delta N)^2 / \langle N \rangle$  is expected to diverge near the critical temperature,  $T_0$ , for the Bose–Einstein condensation, even though finite-size effects, or a repulsive force among bosons, might smoothen the divergence [21]. In our case,  $(\Delta N)^2 / \langle N \rangle < 1$  corresponds to a temperature region around and below the critical point, where a condensate could form.

Significant differences, up to about 2 orders of magnitude, can also be observed between fermions and bosons in the quadrupole

momentum ( $Q_{xy} = p_x^2 - p_y^2$ ) fluctuations for the three studied particles, shown in Fig. 1 (panel d). Within a classical picture these differences can be explained as different temperatures of the QP at the emission of each particle [18] and therefore different time scales of the different particle-types emission [24].

Results obtained from statistical decay models (like GEMINI [19, 25]) are compared to our data and shown in panels (a), (c), and (d) as dotted lines. The GEMINI model typically well reproduces the observables in statistical decay experiments populating nuclei with similar excitation energies [25]. In our case GEMINI reproduces the ordering of the multiplicity (panel a) and the quadrupole momentum fluctuations (panel d) of protons, deuterons and  $\alpha$ s. This is not surprising since these two quantities are related to the reaction Q-value and to the decaying-nucleus excitation energy (and temperature) which are properly accounted for in the model. A fine tuning of the model could even lead to reproduce the observed values. However, this is not the case for the multiplicity fluctuations, whose ordering and values are not reproduced by the model. This is due to the fact that, in the model, the quantum nature of the studied particles, and in particular the bosonic nature of deuterons and  $\alpha$ s, is neglected. These observations indicate that the emission is not compatible with a standard statistical decay. Theoretical approaches accounting for the bosonic nature of deuterons and  $\alpha$ s are currently under development [26,27] and in future these data could be a further benchmark for these models. The influence of the event selection was also investigated all along the analysis and showed that the observed behaviours are not biased by the performed selections.

In this work, in order to track possible Bose-condensation signals, we select  $\alpha$ -conjugate and deuteron-conjugate QP systems by selecting events with a reconstructed quasi-projectile mass  $A_{QP} = 40$ . Being on the one hand aware that mixing events with different number of bosons might affect the experimental analysis of BEC signals and, on the other hand, attempting to increase the statistics, we preferred to handle slightly different selections of events under the constraint that they had to yield to similar results as when  $A_{QP} = 40$  is chosen, within the error bars. In particular, we selected events with  $A_{QP} = 36, 40$  and  $44$  for the analysis involving  $\alpha$  particles, with  $34 \leq A_{QP} \leq 46$  when involving deuterons, and with  $38 \leq A_{QP} \leq 42$  for the case of protons. Both even and odd  $A_{QP}$  values were used in the analysis of deuterons and protons. We have verified all along the analysis that such event class selection leads to results similar to those obtained when selecting  $A_{QP} = 40$  events within the error bars.

The temperatures and mean partial densities of different portions of the colliding systems can be estimated by studying the measured particle quadrupole momentum and multiplicity fluctuations, as well as mean particle multiplicities, according to the method described in [28,29]. The method takes into account the fermionic and bosonic nature of the particles, i.e. fermions and bosons follow the Fermi and Bose statistics, respectively, and their mutual Coulomb repulsion is also accounted for [30]. Including the Coulomb repulsion is crucial especially for the Bose condensate, indeed disregarding this contribution would make the condensate unphysically unstable [21,30]. This leads, for each studied boson (fermion), to two (three) coupled equations with two (three) unknowns: the temperature and the mean volume (and the chemical potential, which is zero for bosons at temperatures below the critical point, as in the present case [21]). In the following we will concentrate on the first two quantities and, in particular, we will discuss the local partial densities of the species of considered particles. Within such approach, each particle species  $i = p, d$  or  $\alpha$  can be associated to a corresponding temperature  $T_i$ . By means of the mean multiplicities  $\langle N \rangle_i$  of particles measured with the INDRA-VAMOS setup, and exploiting momentum-space observables, local

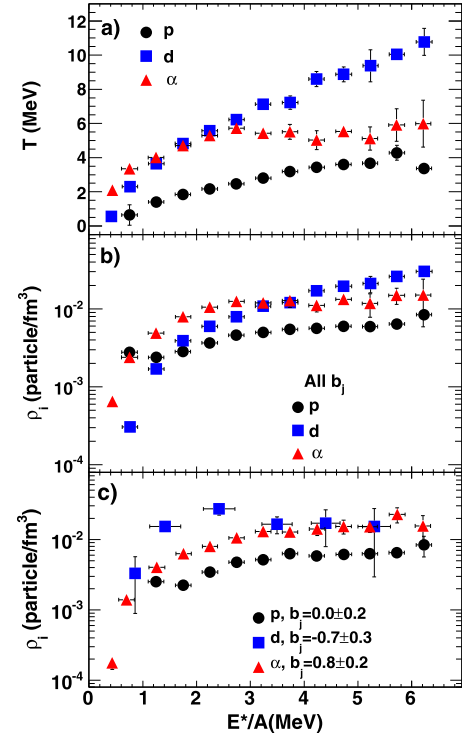
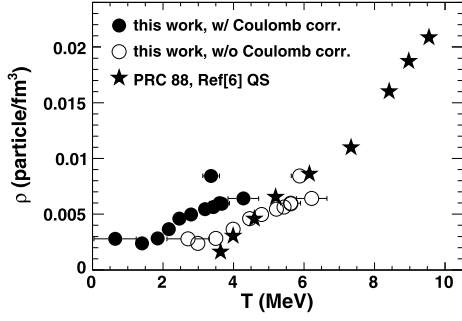


Fig. 2. (Colour online.) (a) Temperatures and (b) local partial densities vs. transverse excitation energy per nucleon extracted from proton, deuteron and  $\alpha$  fluctuations. (c) Same as panel (b) with gates applied on  $b_j$  values (see text).

partial densities  $\rho_i$  could also be estimated for each species of the probe particles.

The temperatures,  $T_i$ , of each probe-particle species are shown in Fig. 2(a) as a function of  $E^*/A$ . The temperature increases with the excitation energy for both protons and deuterons, while we observe a flattening of  $T_i$  above 3 MeV/A excitation energy for  $\alpha$  particles. The performed event selection, and in particular the  $Q_{shape}$  cut, does not impact, within the error bars, the temperatures measured for protons and deuterons, while it lowers the measured temperatures for  $\alpha$  particles of at most 1 MeV for excitation energies above 3 MeV/A, without modifying the trend here displayed. The obtained values of temperature, as well as the observed trends, are similar to previous works performed in similar experimental conditions (see for instance Ref. [18,31] and refs therein) when neglecting in the analysis the Coulomb correction [32]. The study of the influence of this correction on the temperature values can be found in [33]. A detailed study of the temperature behaviour will be the subject of a forthcoming work [34]. Within a classical picture, the significant spread in measured temperatures across fragment types is consistent with the already mentioned ordering in the emission time of the different particles, in agreement with the experimental findings obtained via particle interferometry [24, 35,36].

The local partial densities obtained for the probed particles,  $\rho_i$ , are shown in Fig. 2(b) as a function of  $E^*/A$ . The extracted densities increase as  $E^*/A$  increases for the three probe particles. This behaviour has different interpretations depending on the details of the decay mechanism. At low excitation energies ( $E^* < 2-3$  MeV) the decay most likely proceeds by evaporation, where ejectiles probe a lower surface density as compared to the bulk density of the residue. On the contrary, higher local partial densities  $\rho_i$  are extracted at increasing excitation energy, where multifragment break-up may involve the whole bulk of the system, leading to the coexistence of fragments and light particles ( $Z < 3$ ), commonly



**Fig. 3.** Temperature vs. local partial densities extracted from proton analysis. Data obtained from fluctuations accounting (full circles) and neglecting (empty circles) the Coulomb correction are compared with data reported in Ref. [44] (stars).

associated to a “gas-like” phase. In this case,  $\rho_i$  corresponds to particles  $i$  which are found in the dilute (gas-like) phase produced in the disassembly of the hot QP system [37–41]. In line with the above analysis, similar results on temperatures and on local partial densities of protons could be obtained within a coalescence approach in a quantum-statistical framework including medium effects applied to previous experimental works performed in similar conditions [42–44]. These densities are not modified, within the error bars, by the imposed event selection ( $Q_{\text{shape}}$ ). The comparison of the obtained  $T$  and  $\rho$  values (full circles) to those reported in Ref. [44] (stars) is shown in Fig. 3. Results obtained neglecting in the analysis the Coulomb correction are also plotted (empty circles) to highlight the key role played by this correction in the temperature determination. If we now compare the results shown in Fig. 2(b) for bosons ( $d$  or  $\alpha$ ) and fermions ( $p$ ), we observe that the local partial densities of proton and alpha increases as  $E^*/A$  increases, both saturating at  $\sim 2$  MeV/nucleon around  $4 \times 10^{-3}$  and  $10^{-2}$  particles/fm<sup>3</sup>, respectively. However, the saturation does not occur for deuterons. Their local partial densities are below those extracted for fermions (protons) at low  $E^*$ , while they rise above the local partial densities of  $\alpha$  at higher  $E^*$ . Regardless of their specific behaviour, we observe that the local partial density of fermions is much lower (up to a factor 4) than the local partial densities associated to both boson species for  $E^* > 1$  MeV/nucleon. To illustrate what this finding implies, we assume that a schematic relation holds between the density  $\rho_i$ , the mean distance  $\langle R \rangle_i$  between pairs of particles of the same species and a corresponding volume  $v_i = \langle N \rangle_i / \rho_i \propto R_i^3$ . Then from the observed difference between densities we can deduce, on average, estimates of mean distance between fermions up to  $\sim 60\%$  bigger than the mean distance between bosons. We therefore interpret the observed results as a reduction of the fermionic component where the bosonic one is present and possibly as the appearance of a condensation phenomena occurring in excited nuclear systems. If this is the case, we should also expect boson energy densities higher than the fermion one, and condensation temperatures of the order of few MeV, consistently with [21,30,45]. These behaviours recall what is observed in atomic physics [2]: while bosons seem to condense, experiencing higher densities and smaller relative distances, fermions, due to the Pauli principle, tend to move apart, experiencing lower densities and larger relative distances.

Before presenting the mentioned observables, we remark that each event is a mixture of interacting fermions and bosons. To shed more light on the observations, we separate bosonic-like events and fermionic-like events by means of the event-by-event quantity:

$$b_j = \frac{1}{M} \sum_{i=1}^M \frac{(-1)^{N_i} + (-1)^{Z_i}}{2} \quad (1)$$

where  $M$  is the event multiplicity and  $Z_i$  and  $N_i$  are the charge and neutron numbers of the  $i$ -th fragment, respectively.  $b_j$  is equal to 1,  $-1$  and 0 when all fragments emitted in the event are  $Z$  even- $N$  even,  $Z$  odd- $N$  odd, and  $A$ -odd, respectively. To isolate events mostly dominated by the emission of bosons or fermions [30], we select  $\alpha$ -like,  $p$ -like and  $d$ -like events by applying gates  $b_j = 0.8 \pm 0.2$ ,  $0.0 \pm 0.2$  and  $-0.7 \pm 0.3$ , respectively. Due to lower statistics, we increase the bin size for both  $b_j$  and  $E^*/A$  distributions when selecting  $d$ -like events.

Fig. 2(c) shows the extracted local partial densities,  $\rho_i$ , as a function of excitation energy,  $E^*/A$ , of protons in  $p$ -like events, by deuterons in  $d$ -like events and by alphas in  $\alpha$ -like events. The local partial densities probed by bosons ( $d$  and  $\alpha$ ) are in remarkably good agreement at higher excitation energies and systematically bigger than the density of fermions. Furthermore, we observe that the local partial densities probed by  $\alpha$  and proton in  $\alpha$ -like and  $p$ -like events (panel c) are not different from the ones shown on panel (b) and corresponding to events containing mixtures of bosons and fermions. These observations indicate that bosons experience higher local partial densities as compared to fermions both in purely boson-like events and in events where mixtures of bosons and fermions are emitted. Therefore we interpret them as signals consistent with the possible existence of Bose-condensation phenomena, which seem to persist even in the presence of fermions.

We now study the dependence of the excitation energy per particle, defined as  $E_i = A_i \cdot E^*/A_{\text{QP}}$  where  $A_i$  is the atomic number of the probe-particle species  $i$ , on the temperature  $T_i$  and the local partial density  $\rho_i$  associated to the particle species  $i$ . For the ideal Bose (below the critical temperature,  $T_0$ ) and for the ideal Fermi gases (at low  $T$ )  $E_i$  is proportional to  $T_i^{5/2}/\rho_i$  and  $T_i^2/\rho_i^{2/3}$ , respectively. Such dependence,  $E_i \propto T_i^\beta/\rho_i^\gamma$ , is tested in Fig. 4(a and b) for both mixture and purely boson/fermion-like events, by setting  $\beta = 2$  and  $\gamma = 2/3$  for fermions and  $\beta = 5/2$  and  $\gamma = 1$  for bosons. The expected dependence is satisfied within the error bars by all the probe-particle species  $i$ , confirming their different quantum behaviour in contributing to the density profile. This is the case also when removing the imposed  $Q_{\text{shape}}$  constraint.

To compare the different cases, we study the total energy density, defined as  $\varepsilon_{t,i} = (E^* + m_i)/V_i$ , as a function of the temperature  $T_i$  for both mixture and purely boson/fermion-like events (Fig. 4(c)–(d)). The total energy density is always larger for bosons than for fermions. In the case of the mixture it is striking to observe that the total energy densities obtained for different bosons are in remarkably good agreement, and they are higher than those obtained for fermions by about a factor 7, independently of the temperature. This signal is present independently of the performed event selection. A similar behaviour and similar values of  $\varepsilon_{t,i}$  are observed for  $\alpha$ s and protons when considering boson and fermion-like events, thus confirming our previous observations. The values obtained for deuterons when considering boson-like events are affected by large error bars, thus making the interpretation of the results difficult.

For an ideal Bose gas we can derive the critical temperature  $T_0$  from  $E_i$  [21]. The results are presented in Fig. 5 as a function of the local partial density of  $\alpha$ s and  $d$  for both mixture and boson-like events (the lines indicate the ideal boson gas result). Values of the order of a few MeV’s are obtained for both particles, in agreement with theoretical predictions for condensation temperatures [30,45] and independently of the event selection. As expected, the experimentally derived values are systematically higher both for  $d$  and  $\alpha$  as compared to the ideal case. Indeed, the Coulomb repulsion enhances the condensation [28–30,45,46], thus resulting in higher  $T_0$  as compared to the ideal case. This is very similar to



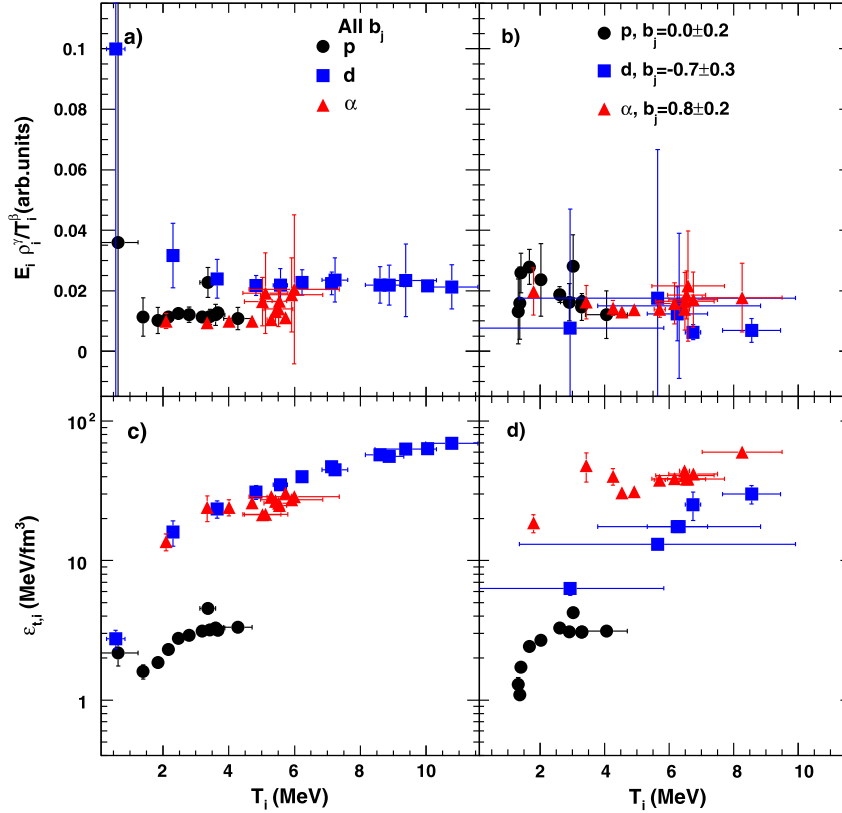


Fig. 4. (Colour online.) (a)  $E_i \rho_i^\gamma / T_i^\beta$  (see text) and (c) total energy density as function of temperatures for mixture (a)–(c) and (b)–(d) pure boson/fermion-like events.

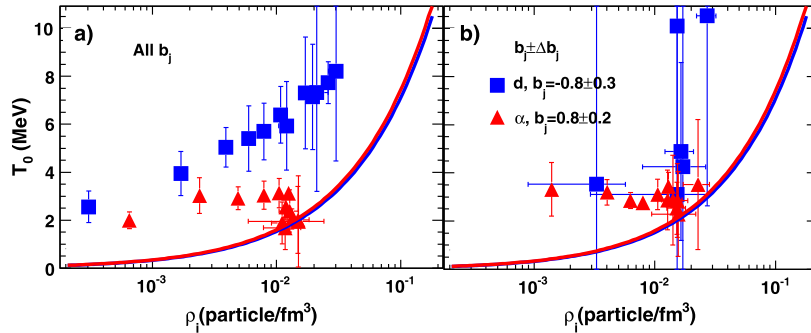


Fig. 5. (Colour online.) Critical temperature vs local partial density for (a) mixture and (b) boson-like events.

what has been found in traps [45], and was also predicted theoretically [30,32]. It is important to remark that at high densities, and especially for the  $\alpha$  case ( $d$  displays unfortunately large error bars due to poor statistics), the data are closer to the ideal case. This is due to the increased contribution of the nuclear force in counterbalancing the Coulomb repulsion. As suggested in Ref. [47], we expect that at even higher densities the attractive nuclear force becomes dominant, the bosons overlap and dissolve into their constituent fermions ( $p$  and  $n$ ) and the Pauli blocking becomes dominant.

In summary, we have studied the decay of excited quasi-projectile systems produced in mid-peripheral  $^{40}\text{Ca} + ^{40}\text{Ca}$  collisions at  $E/A = 35$  MeV with the INDRA-VAMOS setup. Within the selected events, local partial densities and temperatures probed by bosons (deuterons and alphas) and by fermions (protons) in the low density gas-like phase have been estimated with quantum-fluctuation methods. The observed results show that bosons experience a higher density and a higher energy density than fermions.

These results indicate a reduction of the fermionic component where the bosonic one is present, in favour of conditions which may be associated to the presence of Bose condensation and Fermi quenching phenomena in nuclear systems. Condensation temperatures are in agreement with theoretical predictions. These phenomena are observed even in events where mixtures of bosons and fermions coexist, suggesting that they are not reduced by boson-fermion interactions. The results of this work recall similar phenomena observed in atomic systems where the coexistence of a quasi-pure Bose-Einstein condensate of  $^7\text{Li}$  atoms (bosons) in a Fermi sea of  $^6\text{Li}$  (fermions) was observed [2]. This interdisciplinary analogy seems to indicate a similar nature for processes occurring in quantum systems at the atomic and nuclear scale, regardless of their different sizes and characteristic interactions. Future investigations on implications of these phenomena on  $\alpha$  clustering and symmetry energy at low density [26,27,48–50] stimulate using also particle-particle correlations [24] to estimate emission densities and volumes, even in more central collisions.

## Acknowledgements

We thank the staff of the GANIL Accelerator facility for their support during the experiment. We also gratefully acknowledge the collaboration of M. Rejmund, A. Navin and F. Farget which made the experiment successful. This work was supported by le Commissariat à l'Énergie Atomique et aux énergies alternatives, le Centre Nationale de la Recherche Scientifique, le Ministère de l'Éducation Nationale, and le Conseil Régional de Basse Normandie.

## References

- [1] C. Ebner, D. Edwards, *Phys. Rep.* 2 (2) (1971) 77–154.
- [2] F. Schreck, L. Khaykovich, K.L. Corwin, G. Ferrari, T. Bourdel, J. Cubizolles, C. Salomon, *Phys. Rev. Lett.* 87 (2001) 080403.
- [3] J.A. Scarpaci, M. Fallot, D. Lacroix, M. Assié, L. Lefebvre, N. Frascaria, D. Beaumel, C. Bhar, Y. Blumenfeld, A. Chbihi, P. Chomaz, P. Desesquelles, J. Frankland, H. Idbarkach, E. Khan, J.L. Laville, E. Plagnol, E.C. Pollacco, P. Roussel-Chomaz, J.C. Roynette, A. Shrivastava, T. Zerguerras, *Phys. Rev. C* 82 (2010) 031301.
- [4] M. Freer, *Prog. Phys.* 70 (2007) 2149.
- [5] Y. Kanada-En'yo, *Phys. Rev. C* 89 (2014) 024302.
- [6] G. Bertsch, W. Bertozzi, *Nucl. Phys. A* 165 (1971) 199, and the references therein.
- [7] Y. Fujiwara, H. Horiuchi, K. Ikeda, M. Kamimura, K. Kato, Y. Suzuki, E. Uegaki, *Prog. Theor. Phys. Suppl.* 68 (1980) 29, and the references therein.
- [8] T. Yamada, P. Schuck, *Phys. Rev. C* 69 (2004) 024309.
- [9] A. Bonasera, M. Bruno, P. Mastinu, C. Dorso, *Riv. Nuovo Cimento* 23 (2000) 1.
- [10] J.B. Natowitz, G. Röpke, S. Typel, D. Blaschke, A. Bonasera, K. Hagel, T. Klähn, S. Kowalski, L. Qin, S. Shlomo, R. Wada, H.H. Wolter, *Phys. Rev. Lett.* 104 (2010) 202501.
- [11] Y.K. Gambhir, P. Ring, P. Schuck, *Phys. Rev. Lett.* 51 (1983) 1235–1238.
- [12] W. von Oertzen, *Lect. Notes Phys.* 818 (2010) 109.
- [13] J. Pouthas, B. Borderie, R. Dayras, E. Plagnol, M. Rivet, F. Saint-Laurent, J. Steckmeyer, G. Auger, C. Bacri, S. Barbey, A. Barbier, A. Benkirane, J. Benlliure, B. Berthier, E. Bougamont, P. Bourgault, P. Box, R. Bzyl, B. Cahlan, Y. Cassagnou, D. Charlet, J. Charvet, A. Chbihi, T. Clerc, N. Copinet, D. Cussol, M. Engrand, J. Gautier, Y. Hugué, O. Jouniaux, J. Laville, P.L. Botlan, A. Leconte, R. Legrain, P. Lelong, M.L. Guay, L. Martina, C. Mazur, P. Mosrin, L. Olivier, J. Passerieux, S. Pierre, B. Piquet, E. Plaige, E. Pollacco, B. Raine, A. Richard, J. Ropert, C. Spitaels, L. Stab, D. Sznajderman, L. Tassan-got, J. Tillier, M. Tripon, P. Vallerand, C. Volant, P. Volkov, J. Wieleczko, G. Wittwer, *Nucl. Instrum. Methods Phys. Res. A* 357 (1995) 418–442.
- [14] H. Savajols, VAMOS Collaboration, *Nucl. Instrum. Methods Phys. Res. B* 204 (2003) 146.
- [15] P. Marini, B. Borderie, A. Chbihi, N. Le Neindre, M.-F. Rivet, J.P. Wieleczko, M. Zoric, et al., (INDRA-VAMOS Collaboration). Exploring isospin effects on the level density and the density dependence of the symmetry energy, in: J.D. Frankland (Ed.), *Proceedings of the IWM2009 International Workshop on Multifragmentation, and Related Topics*, 2010, p. 189 and the references therein.
- [16] J. Steckmeyer, E. Genouin-Duhamel, E. Vient, J. Colin, D. Durand, G. Auger, C. Bacri, N. Bellaize, B. Borderie, R. Bourgault, B. Bouriquet, R. Brou, P. Buchet, J. Charvet, A. Chbihi, D. Cussol, R. Dayras, N.D. Cesare, A. Demeyer, D. Doré, J. Frankland, E. Galichet, E. Gerlic, D. Guinet, S. Hudan, P. Loutesse, F. Lavaud, J. Laville, J. Lecolley, C. Leduc, R. Legrain, N.L. Neindre, O. Lopez, M. Louvel, A. Maskay, L. Nalpas, J. Normand, M. Parlog, P. Pawlowski, E. Plagnol, M. Rivet, E. Rosato, F. Saint-Laurent, G. Tabacaru, B. Tamain, L. Tassan-Got, O. Tirel, K. Turzo, M. Vigilante, C. Volant, J. Wieleczko, *Nucl. Phys. A* 686 (2001) 537–567.
- [17] P. Marini, A. Zarrella, A. Bonasera, G. Bonasera, P. Cammarata, L. Heilborn, Z. Kohley, J. Mabilia, L. May, A. McIntosh, A. Raphelt, G. Souliotis, S. Yennello, *Nucl. Instrum. Methods Phys. Res. A* 707 (2013) 80–88.
- [18] S. Wuenschel, A. Bonasera, L. May, G. Souliotis, R. Tripathi, S. Galanopoulos, Z. Kohley, K. Hagel, D. Shetty, K. Huseman, S. Soisson, B. Stein, S. Yennello, *Nucl. Phys. A* 843 (2010) 1.
- [19] R. Charity, M. McMahan, G. Wozniak, R. McDonald, L. Moretto, D. Sarantites, L. Sobotka, G. Guarino, A. Pantaleo, L. Fiore, A. Gobbi, K. Hildenbrand, *Systematics of complex fragment emission in niobium-induced reactions*, *Nucl. Phys. A* 483 (1988) 371–405.
- [20] E. Bonnet, B. Borderie, N.L. Neindre, M. Rivet, R. Bourgault, A. Chbihi, R. Dayras, J. Frankland, E. Galichet, F. Gagnon-Moisan, D. Guinet, P. Loutesse, J. Lukasik, D. Mercier, M. Parlog, E. Rosato, R. Roy, C. Sfienti, M. Vigilante, J.B.Z. Wieleczko, INDRA Collaboration, *Nucl. Phys. A* 816 (2009) 1–18, and the references therein.
- [21] L. Landau, F. Lifshits, *Statistical Physics*, Pergamon, New York, 1980.
- [22] C. Sanner, E.J. Su, A. Keshet, R. Gommers, Y.-i. Shin, W. Huang, W. Ketterle, *Suppression of density fluctuations in a quantum degenerate Fermi gas*, *Phys. Rev. Lett.* 105 (2010) 040402.
- [23] B.C. Stein, A. Bonasera, G.A. Souliotis, H. Zheng, P.J. Cammarata, A.J. Echeverria, L. Heilborn, A.L. Keksis, Z. Kohley, J. Mabilia, P. Marini, L.W. May, A.B. McIntosh, C. Richers, D.V. Shetty, S.N. Soisson, R. Tripathi, S. Wuenschel, S.J. Yennello, *J. Phys. G, Nucl. Part. Phys.* 41 (2014) 025108.
- [24] G. Verde, A. Chbihi, R. Ghetti, J. Helgesson, *Eur. Phys. J. A* 30 (2006) 81–108.
- [25] R.J. Charity, *Phys. Rev. C* 82 (2010) 014610, and the references therein.
- [26] S. Typel, G. Röpke, T. Klähn, D. Blaschke, H.H. Wolter, *Phys. Rev. C* 81 (2010) 015803.
- [27] S. Typel, *Phys. Rev. C* 89 (2014) 064321.
- [28] H. Zheng, G. Giuliani, A. Bonasera, *Nucl. Phys. A* 892 (2012) 43–57.
- [29] H. Zheng, A. Bonasera, *Phys. Lett. B* 696 (2011) 178–181; H. Zheng, A. Bonasera, *Phys. Rev. C* 86 (2012) 027602.
- [30] H. Zheng, G. Giuliani, A. Bonasera, *Phys. Rev. C* 88 (2013) 024607, arXiv: 1305.5494.
- [31] A. Chbihi, O. Schapiro, S. Salou, D.H.E. Gross, *Eur. Phys. J. A* 5 (1999) 251.
- [32] H. Zheng, G. Giuliani, A. Bonasera, *J. Phys. G, Nucl. Part. Phys.* 41 (2014) 055109.
- [33] J. Mabilia, H. Zheng, A. Bonasera, P. Cammarata, K. Hagel, L. Heilborn, Z. Kohley, L.W. May, A.B. McIntosh, M.D. Youngs, A. Zarrella, S.J. Yennello, *Phys. Rev. C* 90 (2014) 027602.
- [34] P. Marini, et al., in preparation.
- [35] R. Ghetti, J. Helgesson, V. Avdeichikov, P. Golubev, B. Jakobsson, N. Colonna, G. Tagliente, S. Kopecky, V.L. Kravchuk, H.W. Wilschut, E.W. Anderson, P. Nadel-Turonski, L. Westerberg, V. Bellini, M.L. Sperduto, C. Sutura, *Phys. Rev. Lett.* 91 (2003) 092701.
- [36] D. Gourio, D. Ardouin, M. Assenard, G. Auger, C. Bacri, N. Bellaize, A. Benkirane, J. Benlliure, B. Berthier, E. Bisquer, B. Borderie, R. Bourgault, P. Box, R. Brou, J. Charvet, A. Chbihi, J. Colin, D. Cussol, R. Dayras, E. De Filippo, A. Demeyer, C. Donnet, D. Durand, P. Ecomard, P. Eudes, M. Germain, D. Guinet, L. Lakehal-Ayat, P. Loutesse, J. Laville, L. Lebreton, C. Le Brun, J. Lecolley, T. Lefort, A. Lefèvre, R. Legrain, N. Le Neindre, O. Lopez, M. Louvel, N. Marie, V. Métivier, L. Nalpas, A. Ouatzerga, M. Parlog, J. Péter, E. Plagnol, E. Pollaco, A. Rahmani, R. Régimbart, T. Reposeur, M. Rivet, E. Rosato, F. Saint-Laurent, S. Salou, M. Squallii, J. Steckmeyer, G. Tabacaru, B. Tamain, L. Tassan-Got, E. Vient, C. Volant, J. Wieleczko, A. Wieloch, K. Yuasa-Nakagawa, *Eur. Phys. J. A, Hadrons Nucl.* 7 (2000) 245.
- [37] L.G. Moretto, K.A. Bugaev, J.B. Elliott, R. Ghetti, J. Helgesson, L. Phair, *Phys. Rev. Lett.* 94 (2005) 202701.
- [38] L.G. Moretto, J.B. Elliott, L. Phair, P.T. Lake, The experimental liquid–vapor phase diagram of bulk nuclear matter, *J. Phys. G, Nucl. Part. Phys.* 38 (2011) 113101.
- [39] E.A. Guggenheim, *J. Chem. Phys.* 13 (1945) 253.
- [40] J.B. Elliott, L.G. Moretto, L. Phair, G.J. Wozniak, L. Beaulieu, H. Breuer, R.G. Korteling, K. Kwiatkowski, T. Lefort, L. Pienkowski, A. Ruangma, V.E. Viola, S.J. Yennello, *Phys. Rev. Lett.* 88 (2002) 042701.
- [41] J.B. Elliott, P.T. Lake, L.G. Moretto, L. Phair, *Phys. Rev. C* 87 (2013) 054622.
- [42] S. Kowalski, J.B. Natowitz, S. Shlomo, R. Wada, K. Hagel, J. Wang, T. Materna, Z. Chen, Y.G. Ma, L. Qin, A.S. Botvina, D. Fabris, M. Lunardon, S. Moretto, G. Nebbia, S. Pesente, V. Rizzi, G. Viesti, M. Cinausero, G. Prete, T. Keutgen, Y.E. Masri, Z. Majka, A. Ono, *Phys. Rev. C* 75 (2007) 014601.
- [43] L. Qin, K. Hagel, R. Wada, J.B. Natowitz, S. Shlomo, A. Bonasera, G. Röpke, S. Typel, Z. Chen, M. Huang, J. Wang, H. Zheng, S. Kowalski, M. Barbui, M.R.D. Rodrigues, K. Schmidt, D. Fabris, M. Lunardon, S. Moretto, G. Nebbia, S. Pesente, V. Rizzi, G. Viesti, M. Cinausero, G. Prete, T. Keutgen, Y. El Masri, Z. Majka, Y.G. Ma, *Phys. Rev. Lett.* 108 (2012) 172701.
- [44] G. Röpke, S. Shlomo, A. Bonasera, J.B. Natowitz, S.J. Yennello, A.B. McIntosh, J. Mabilia, L. Qin, S. Kowalski, K. Hagel, M. Barbui, K. Schmidt, G. Giuliani, H. Zheng, S. Wuenschel, *Phys. Rev. C* 88 (2013) 024609.
- [45] R.P. Smith, R.L.D. Campbell, N. Tammuz, Z. Hadzibabic, *Phys. Rev. Lett.* 106 (2011) 250403.
- [46] K. Huang, *Statistical Mechanics*, Second edition, John Wiley & Sons, 1987, p. 286, 294, and following.
- [47] G. Röpke, *Phys. Rev. C* 92 (2015) 054001, and the references therein.
- [48] S. Typel, H. Wolter, G. Röpke, D. Blaschke, *Eur. Phys. J. A* 50 (2014) 17.
- [49] M. Girod, P. Schuck, *Phys. Rev. Lett.* 111 (2013) 132503.
- [50] M. Hempel, K. Hagel, J. Natowitz, G. Röpke, S. Typel, *Phys. Rev. C* 91 (2015) 045805.